EUROPHYSICS LETTERS 1 August 1992

Europhys. Lett., **19** (7), pp. 629-635 (1992)

Neutron Spectroscopy and Electron-Phonon Coupling in Alkali-Metal–Doped Fullerides.

K. PRASSIDES (*), C. CHRISTIDES (*), M. J. ROSSEINSKY (**), J. TOMKINSON (***) D. W. MURPHY (**) and R. C. HADDON (**)

(*) *School of Chemistry and Molecular Sciences, University of Sussex Brighton BN1 9QJ, UK*
(**) *AT&T Bell Laboratories - Murray Hill, NJ 07974, USA*
(***) *Rutherford Appleton Laboratory - Didcot, Oxon OX11 0QX, UK*

(received 1 April 1992; accepted in final form 7 July 1992)

PACS. 74.70J – Superconducting layer structures and intercalation compounds.
PACS. 25.40F – Inelastic neutron scattering and (n, p) reactions.

Abstract. – The vibrational spectrum of saturation-doped insulating Rb_6C_{60} has been measured by inelastic neutron scattering at nonzero momentum transfer in the energy range (5 ÷ 200) meV at 20 K. The two lowest-energy fivefold degenerate H_g modes sharpen substantially in comparison with superconducting K_3C_{60}, acquiring comparable widths to those found in pristine C_{60}. This is interpreted as evidence for the importance of these modes in the pairing interaction for superconductivity. We estimate that the radial H_g modes make a substantial contribution to the total electron-phonon coupling strength in the superconducting fullerides.

Introduction. – Unlike semi-metallic graphite, pristine C_{60} is a poor conductor with a band gap of ≈ 1.9 eV. However, intercalation of alkali metals into the f.c.c. crystal structure leads to an increase in electrical conductivity of several orders of magnitude [1] and the appearance of superconductivity [2] at critical temperatures considerably higher than the analogous graphite intercalates [3]. The superconducting A_3C_{60} [4] phases have T_c's increasing with the unit cell size [5] to over 30 K. Insulating A_2C_{60}, A_4C_{60} and A_6C_{60} [6] phases have also been isolated. Superconductivity has been interpreted in terms of either electronic [7] or phonon-mediated pairing [8-12]. The electron-phonon–based theories have employed either low-energy A^+-C_{60} optic [8] or high-energy [9-12] intramolecular modes. Furthermore, the relative role of the intramolecular modes emerges differently from the various calculations performed: i) coupling strength is found to be distributed almost equally among radial and tangential modes [9], and ii) either the highest-energy tangential [10] or the lowest-energy radial modes [11] alone are found to contribute principally to the electron-phonon interaction. Strong support for phonon-mediated pairing involving carbon vibrations, but with significant Coulomb interaction effects has come from isotope-effect measurements in ^{13}C-substituted A_3C_{60} [13]. Neutron scattering measurements at nonzero $|Q|$ on C_{60} [14] and K_3C_{60} [15] have revealed that selected radial and tangential vibrations of H_g symmetry broaden substantially in the superconductor and are strongly involved in the pairing interaction. Similar supporting evidence has come from Raman measurements on superconducting fulleride films [16]; these

also show that the low-frequency $H_g^{(1)}$ mode exhibits a Breit-Wigner lineshape and the intramolecular frequencies do not vary between K_6C_{60} and Rb_6C_{60}.

We now report inelastic neutron scattering (INS) measurements away from the Brillouin zone centre on the saturation-doped insulating fulleride Rb_6C_{60} in the energy range $(5 \div 200)$ meV at 20 K. We find that intramolecular vibrational modes, like $H_g^{(1)}$ and $H_g^{(2)}$, sharpen significantly when compared to superconducting K_3C_{60} [15], their full widths at half-maximum being comparable to those in pristine C_{60} [14]. This constitutes strong evidence that the broadening effects observed in K_3C_{60} do not arise because of cage reduction $C_{60} \rightarrow C_{60}^{3-} \rightarrow C_{60}^{6-}$, or K^+ disorder introduced by intercalation, but reflect electron-phonon coupling. We also present a quantitative estimation of the electron-phonon coupling strengths λ_i of the radial H_g modes; our results are consistent with a large contribution to the total electron-phonon coupling constant originating from the two lowest-energy H_g modes $(H_g^{(1)}, H_g^{(2)})$.

Experimental. – Rb_6C_{60} was prepared by reaction of C_{60} with Rb metal in a sealed, evacuated pyrex tube at 250 °C (4 days), 300 °C (4 days), followed by distillation of excess Rb away from the product. Phase purity was confirmed by X-ray and neutron diffraction. INS measurements in down-scattering mode on a 600 mg sample, sealed in a 9 mm diameter silica tube under 0.5 atm. He, were performed between 5 and 200 meV at 20 K using a closed-cycle He refrigerator, with the Time-Focused Crystal Analyser (TFXA) spectrometer at the ISIS Facility, UK; a background run was recorded on an identical silica tube. TFXA is an inverted-geometry white-beam spectrometer with a $\Delta\omega/\omega \leqslant 2\%$ resolution, achieved by using a small final neutron energy ($E_f \approx 4$ meV). The cut in (Q, ω) space followed by the detectors is defined by the relationship: $Q^2 = k_i^2 + k_f^2 - 2k_i k_f \cos\phi$, where k_i and k_f are the initial and final neutron wave vectors related to the initial and final energies by: $E_{i,f} = \hbar^2 k_{i,f}^2/2m$ and $\phi = 135°$ is the scattering angle. There is little momentum transfer Q variation at a particular energy transfer $\omega = E_i - E_f$. As a result of large Debye-Waller factors at large ω, high-energy ($\geqslant 150$ meV) spectral features may be partially washed out. The instrumental characteristics permit the use of the incoherent approximation at energy transfers $\geqslant 25$ meV, even for coherent scatterers like carbon. INS measurements are not restricted by the usual optical selection rules and the full vibrational spectrum of C_{60}^{6-} containing information on all 46 normal modes is obtained. In addition, there is information on the intermolecular low-energy modes. The intramolecular modes show no significant dispersion (except at low energies, where dispersion up to 2.5 meV [17] is predicted), permitting direct comparisons between our data, collected at points throughout the Brillouin zone and the available zone-centre theoretical and experimental data to be made. INS measurements are not affected by optical-penetration-depth problems, important in optical spectroscopy.

Results. – The vibrational spectrum of Rb_6C_{60} (cf. C_{60} [14, 18], K_3C_{60} [15], Rb_3C_{60} [19]) may be divided into two regions: i) $(0 \div 25)$ meV (fig. 1*a*)), corresponding to intermolecular and Rb^+-C_{60}^{6-} optic modes and ii) $(25 \div 200)$ meV (fig. 1*b*)), corresponding to intramolecular modes (table I). We also include in fig. 1*b*) the variation of the scattering law $S(Q, \omega)$ with momentum transfer Q. The low-energy region is characterised by two fairly sharp features at 6.4(2) and 8.4(2) meV, possibly associated with translational/librational phonons and a broad band at 13.1(3) meV (FWHM = 3.8(6) meV), associated with the intermolecular phonons and the Rb^+-C_{60}^{6-} optic modes. This is to be compared with K_3C_{60}, which has a sharp librational/translational feature at 4.3 meV and a broad band at 14 meV (FWHM = = 7 meV) [15]. The softening observed for the optic mode may arise from the heavier Rb atom. There is also a large 15 meV gap present in the vibrational spectrum $((18 \div 33)$ meV), separating the internal from the external vibrations. The intramolecular part extends

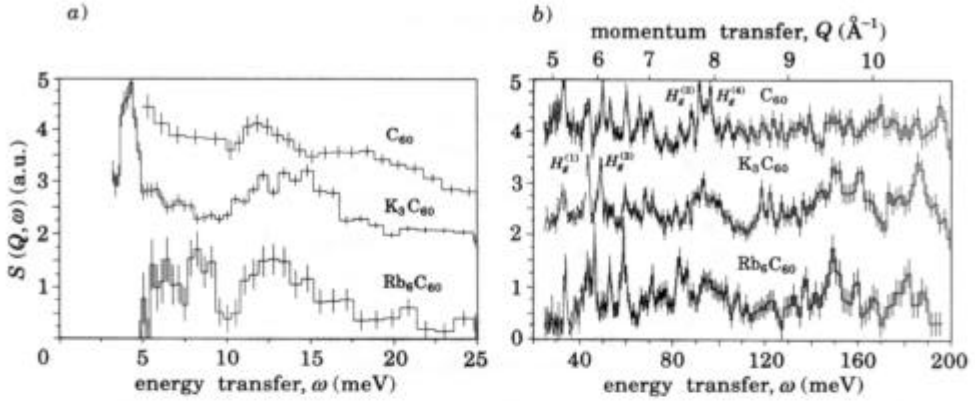

Fig. 1. – Inelastic neutron scattering spectra of Rb_6C_{60} at 20 K (bottom), K_3C_{60} at 5 K (middle) and C_{60} at 20 K (top) in the energy ranges *a*) (0 ÷ 25) meV and *b*) (25 ÷ 200) meV, including the momentum transfer variation. Some assignments in the icosahedral point group I_h are shown.

smoothly from 33 to 190 meV. C_{60} lacks a central atom and radial forces are very weak; the cage vibrations may be further divided into radial ((33 ÷ 110) meV) and tangential ones ((110 ÷ 190) meV). As a result of reduction, the high-energy cut-off in the vibrational DOS softens substantially from 205.0 meV through 198.0 meV (3.4%) to 190.2 meV (7.2%), whereas the low-energy onset is barely affected, showing a hardening (0.8 meV) for C_{60}^{6-}; this reflects the pronounced effect of reduction on the vibrational modes involving stretching components, particularly of the high π-order six-six ring fusions.

Table I lists the positions and (tentative) assignments of some vibrational modes in C_{60}^{n-} ($n = 0, 3, 6$) at low temperatures. An expanded view of the very informative low-energy part of the INS spectra of fig. 1*b*) is shown in fig. 2. Phonon modes are well separated and changes in position and width can be followed as a function of the reduction level of the fullerene cage. For instance, the optically inactive H_u mode softens from 50.0 meV in C_{60} to 49.2 meV in

TABLE I. – *Vibrational spectra of* C_{60} (20 K), K_3C_{60} (5 K) *and* Rb_6C_{60} (20 K) *with tentative assignments. All energies are given in* meV (1 meV = 8.066 cm^{-1}). *Asterisks denote optically active* (IR, *Raman*) *vibrational modes. Assignments of the optically inactive modes are made using the results of the quantum-chemical calculations of Negri et al.* [20].

Assignment	C_{60} ref. [14]	K_3C_{60} ref. [15]	Rb_6C_{60}
$H_g^{(1)*}$	33.1 (1)	32.7 (1)	33.9 (1)
T_{2u}, G_u	42.7 (9), 44.3 (4)	42.2 (4), 43.7 (2)	42.3 (9), 43.4 (4)
H_u	50.0 (1)	49.2 (1)	46.6 (1)
$H_g^{(2)*}$	53.2 (1)	52.5 (2)	53.1 (1)
G_g, A_g^*	60.3 (1)	59.9 (2)	59.1 (1)
T_{1u}^*, $(H_u)(?)$	66.1 (2), (68.6)	63.6 (6), 68.5 (2)	66.7 (6), 68.2 (4)
$(T_{1g}, G_g)(?)$, T_{1u}^*	70.7 (3)	71.5 (4)	71.2 (3)
$T_{2g}(?)$	83.4 (3)	81.4 (2)	82.7 (2)
$H_g^{(3)*}$	88.2 (2)	86.5 (2)	85.9 (3)
$H_u(?)$	91.9 (3)	—	—
$H_g^{(4)*}$	96.2 (2)	94.0 (4)	—

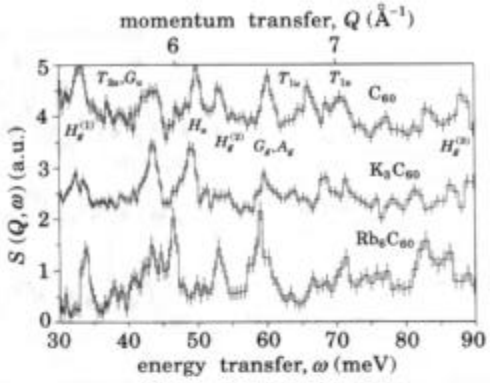

Fig. 2. – Expanded view of the INS spectra of Rb_6C_{60} at 20 K (bottom), K_3C_{60} at 5 K (middle) and C_{60} at 20 K (top) in the energy range (30 ÷ 90) meV, highlighting the changes in the width of the $H_g^{(1)}$ and $H_g^{(2)}$ modes.

K_3C_{60} and 46.6 meV in Rb_6C_{60}; this is proportionately a larger decrease (6.8%) in energy than in the high-energy A_g mode, commonly used to monitor the oxidation level of the fullerene skeleton [1, 16]. We have reported earlier [15] the virtual disappearance, due to broadening, of the $H_g^{(2)}$ phonon of pristine C_{60} at 53.2 meV in superconducting K_3C_{60}. We now find (fig. 2) that this mode sharpens dramatically as we move to insulating Rb_6C_{60}; it softens only marginally to 53.1 meV and its FWHM of 1.4(1) meV is unchanged from C_{60} (FWHM = = 1.3(1) meV). By a fortunate coincidence, $H_g^{(2)}$ occurs in a part of the spectrum uncontaminated by other phonon modes, making our experimental observations and analysis for this mode *unambiguous*. Figure 2 also reveals that the well-isolated $H_g^{(1)}$ mode at 33.9 meV sharpens significantly, compared to that of K_3C_{60}. It also shows a slightly smaller FWHM (1.3(2) meV) than undoped C_{60} (1.7(3) meV), possibly reflecting reduced dispersion effects. At the moment, it is impossible to extract reliable experimental linewidths for the H_g modes in the high-energy region because of the plethora of modes present and the intensity attenuation due to the large Debye-Waller factors.

Discussion and conclusions. – Changes in the phonon DOS of superconducting compounds and their relation to the mechanism of superconductivity are not usually unambiguous, as the extended literature on high-T_c cuprates testifies [21]. However, the molecular nature of the superconducting fullerides results in fairly dispersionless phonon branches and, consequently, simple forms for the electron-phonon Hamiltonian [9, 10]. The total electron-phonon coupling constant λ may be simply expressed as a sum of partial contributions λ_ν, associated with each mode ν mediating the pairing interaction, $\lambda = \sum_\nu \lambda_\nu$. It has been shown, using simple symmetry arguments, that if we consider the t_{1u} electronic states, the only relevant intramolecular modes are the eight H_g and the two A_g (for $k \neq 0$) modes. The phonon linewidths (FWHM) γ_ν, measured directly by neutron scattering, are related to the influence of the electrons on the phonons by: $\gamma_\nu \simeq (\pi/g_\nu)\, N(0)\, \omega_\nu^2 \lambda_\nu$. $N(0)$ is the electronic DOS at the Fermi level, ω_ν the phonon frequency and g_ν the phonon degeneracy. Values of individual mode-coupling constants λ_ν can then be extracted from the observed linewidth changes γ_ν. Table II collects together the values of γ_ν on going from C_{60} to K_3C_{60} for the four lowest-energy H_g modes ($H_g^{(1)}$-$H_g^{(4)}$) which range from 35 cm^{-1} for $H_g^{(2)}$ to 1 cm^{-1} for $H_g^{(3)}$. The exact value of the electronic DOS at the Fermi level has not yet been definitely resolved by experiment; using an estimate of $N(0)$ = 14 states/eV/spin/C_{60} and $g_\nu = 5$, we

TABLE II. – *Observed positions, ω_ν of the four radial H_g modes in C_{60} and their broadenings, γ_ν on reduction to C_{60}^{3-} together with calculated electron-phonon coupling strengths, V_ν in* meV *for a density of states $N(0) = 14$ states/eV/spin/C_{60}. We also include for comparison the values of γ_ν, estimated by the* LDA *frozen phonon calculations of Schluter et al.* [22].

Vibrational mode	$H_g^{(1)}$	$H_g^{(2)}$	$H_g^{(3)}$	$H_g^{(4)}$
ω_ν/meV	33.1	53.2	88.2	96.2
γ_ν/cm^{-1}	8	35	1	25
$\gamma_{\nu,\,calc}$/cm^{-1}	7	15	23	56
V_ν/meV	7.4	12.4	0.1	2.7

can calculate the partial coupling strengths $V_\nu[\equiv \lambda_\nu/N(0)]$. The $H_g^{(2)}$ buckling mode (fig. 3) shows the largest coupling constant, $V_2 = 12.4$ meV. It is followed by $H_g^{(1)}$ which involves a distortion of the spheroidal C_{60} skeleton to an ellipsoid (fig. 3) and has a coupling constant $V_1 = 7.4$ meV. In sharp contrast, $H_g^{(3)}$ shows virtually no change in linewidth, consistent with an insignificant contribution ($V_3 = 0.1$ meV) to the total coupling strength. $H_g^{(4)}$ has a somewhat larger constant $V_4 = 2.7$ meV; however, whereas the three lowest-in-energy modes are well isolated, making extraction of widths unambiguous, $H_g^{(4)}$ overlaps with other vibrational modes. Consequently, we only regard the calculated value of V_4 as approximate. Even though the reported Raman measurements of superconducting fulleride films show considerable differences among themselves, the important role of $H_g^{(1)}$ which shows a Fano lineshape and of $H_g^{(2)}$ in electron-phonon coupling is clearly evident [16].

Information on the λ_ν's may be also extracted through the softening of phonon frequencies due to electron-phonon coupling [22, 9, 10], $\Delta\omega_\nu \approx -(\lambda_\nu \omega_\nu/g_\nu)$. However, changes in *phonon linewidths* are more reliable measures of electron-phonon interactions as energy changes also arise as a result of the cage reduction and depend on details of the electronic structure of the cluster. $H_g^{(1)}$ and $H_g^{(2)}$ show very small changes in frequency ($\approx 1.8\%$ and 1.4%, respectively) consistent with their principally radial character (a softening for K_3C_{60} and a hardening for Rb_6C_{60}, table I, are observed) and in rough agreement with the values expected from electron-phonon coupling arguments. On the other hand, $H_g^{(3)}$ and $H_g^{(4)}$ soften much more than would have been expected from electron-phonon interactions alone (table I, $\approx 1.9\%$ and 2.1%, respectively), consistent with increased tangential character.

The electron-phonon coupling strength is found to be substantial for the radial H_g modes with a cumulative value of $V_{(1\text{-}4)} = \sum_{\nu=1}^{4} V_\nu = 22.6$ meV. This contrasts with models which find or assume that tangential modes will dominate the electron-phonon interaction [10, 12] and provides support for models predicting important contributions from buckling modes [9, 11].

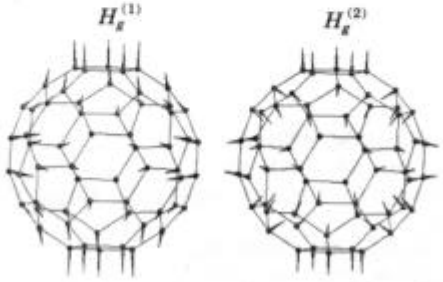

Fig. 3. – Schematic representation of the two lowest-in-energy H_g modes of the C_{60} cage, using the eigenvectors of ref. [17].

In table II, we include the values of the phonon linewidths, $\gamma_{\nu,\,\mathrm{calc}}$ calculated within the framework of Schluter *et al.*'s model which employs a bond charge model [17] and LDA frozen phonon calculations [9, 22]. Even though the detailed comparison with experiment is not perfect, the coupling strength $V_{(1\text{-}4)}$ calculated for the radial modes is only $\approx 10\%$ over our estimated one. The predicted coupling strength for the tangential modes is $V_{(5\text{-}8)} = \sum_{\nu=5}^{8} V_\nu =$ $= 23.0\,\mathrm{meV}$. Taking this value of $V_{(5\text{-}8)}$ as an estimate of the coupling strength in this energy region and combining it with our $V_{(1\text{-}4)}$ value, we obtain a total electron-phonon coupling constant, $V = 45.6\,\mathrm{meV}$. For illustrative purposes, we estimate the value of T_c using McMillan's expression [23]: $T_c = (\omega_{\log}/1.2)\exp[-1.04(1+\lambda)/(\lambda - \mu^*(1+0.62\lambda))]$. The logarithmic mean-phonon-frequency is defined by

$$\omega_{\log} = \exp\left[(1/\lambda)\sum_\nu \lambda_\nu \ln \omega_\nu\right]$$

and μ^* is the phonon-renormalised Coulomb interaction parameter. λ is explicitly related to the magnitude of the DOS at ε_F; using $N(0) = 14$ states/eV/C_{60}/spin, we find $\lambda = 0.64$, a typical size of λ for many weak-coupling superconductors and in excellent agreement with the value extracted from isotope effect measurements [13]. $\omega_{\log}$ is estimated to be 1072 K, 30% smaller than what is usually assumed, reflecting the large partial λ_ν's found for the low-energy modes. Using $\mu^* = 0.15$ [13], T_c is $\approx 17\,\mathrm{K}$, in good agreement with experiment.

In conclusion, we have reported the INS spectrum at $|Q| \neq 0$ of saturation-doped C_{60} at 20 K and combined our results with earlier work on C_{60} and superconducting K_3C_{60} to estimate the contribution of the radial modes to the total electron-phonon coupling strength in the fullerides, $V_{(1\text{-}4)} = 22.6\,\mathrm{meV}$. Our results are consistent with weak-coupling superconductivity, in agreement with isotope-effect measurements and intramolecular electron-phonon coupling theories and can explain the unusually high T_c's observed in the fullerides without invoking any unusual or exotic interactions; *the radial modes are important as a result of simple geometrical reasons*, namely the finite curvature of the fullerene skeleton [9] allows finite σ-π orbital mixing. Such an effect is absent from the corresponding alkali-metal graphite intercalates where the graphitic sheets are strictly flat and provides a rationale for the markedly different T_c's observed in the two types of compounds.

* * *

We thank M. SCHLUTER for valuable discussions and R. M. FLEMING, R. M. LINDSTROM and R. L. PAUL for the sample characterisation. We acknowledge SERC, UK for financial support (KP) and access to ISIS.

REFERENCES

[1] HADDON R. C. *et al.*, *Nature*, **350** (1991) 320.
[2] HEBARD A. F. *et al.*, *Nature*, **350** (1991) 660.
[3] HANNAY N. B. *et al.*, *Phys. Rev. Lett.*, **14** (1965) 225.; KOIKE Y. and TANUMA S., *Solid State Commun.*, **27** (1978) 623.
[4] STEPHENS P. W. *et al.*, *Nature*, **351** (1991) 632.
[5] FLEMING R. M. *et al.*, *Nature*, **352** (1991) 787.
[6] ROSSEINSKY M. J. *et al.*, *Nature*, **356** (1992) 416; FLEMING R. M. *et al.*, *Nature*, **352** (1991) 701; ZHOU O. *et al.*, *Nature*, **351** (1991) 462.

[7] CHAKRAVARTY S. and KIVELSON S., *Europhys. Lett.*, **16** (1991) 751; BASKARAN G. and TOSATTI E., *Curr. Sci.*, **61** (1991) 33; ANDERSON P. W., to be published.
[8] ZHANG F. C., OGATA M. and RICE T. M., *Phys. Rev. Lett.*, **67** (1991) 3452.
[9] SCHLUTER M. A. *et al.*, *Phys. Rev. Lett.*, **68** (1992) 526.
[10] VARMA C. M., ZAANEN J. and RAGHAVACHARI K., *Science*, **254** (1991) 989.
[11] JISHI R. A. and DRESSELHAUS M. S., *Phys. Rev. B*, **45** (1992) 2597.
[12] PIETRONERO L., *Europhys. Lett.*, **17** (1992) 365; MAZIN I. I. *et al.*, *Phys. Rev. B*, **45** (1992) 5114.
[13] RAMIREZ A. P. *et al.*, *Phys. Rev. Lett.*, **68** (1992) 1058; CHEN C. C. and LIEBER C. M., *J. Am. Chem. Soc.*, **114** (1992) 3141; EBBESEN T. W. *et al.*, *Nature*, **355** (1992) 620.
[14] PRASSIDES K. *et al.*, *Chem. Phys. Lett.*, **187** (1991) 455.
[15] PRASSIDES K. *et al.*, *Nature*, **354** (1991) 462.
[16] DUCLOS S. J. *et al.*, *Science*, **254** (1991) 1625; MITCH M. G. *et al.*, *Phys. Rev. Lett.*, **68** (1992) 883; DANIELI R. *et al.*, *Solid State Commun.*, **81** (1992) 257; ZHOU P. *et al.*, *Phys. Rev. B*, **45** (1992) 10838.
[17] ONIDA G. and BENEDEK G., *Europhys. Lett.*, **18** (1992) 403.
[18] CAPPELLETTI R. L. *et al.*, *Phys. Rev. Lett.*, **66** (1991) 3261; COULOMBEAU C. *et al.*, *J. Phys. Chem.*, **96** (1992) 22.
[19] WHITE J. W. *et al.*, *Chem. Phys. Lett.*, **191** (1992) 92.
[20] NEGRI F. *et al.*, *Chem. Phys. Lett.*, **144** (1988) 31; **190** (1992) 174.
[21] ROSSEINSKY M. J. *et al.*, *Phys. Rev. B*, **37** (1988) 2231; RENKER B. *et al.*, *Z. Phys. B*, **67** (1987) 15; RENKER B. *et al.*, *Z. Phys. B*, **73** (1988) 39; CURRAT R. *et al.*, *Phys. Rev. B*, **40** (1989) 11362; PRASSIDES K. *et al.*, *J. Phys. Condens. Matter*, **4** (1992) 965.
[22] SCHLUTER M. A., personal communication.
[23] MCMILLAN W. L., *Phys. Rev.*, **167** (1968) 331.